第 32 卷 第 10 期
2017 年 10 月

无 机 材 料 学 报
Journal of Inorganic Materials

Vol. 32 No. 10
Oct., 2017

Synthesis of AlN Powder by Carbothermal Reduction-nitridation of Alumina/Carbon Black Foam

MAO Xi-Xi[1,2,3], LI Jun[1], ZHANG Hai-Long[2], XU Yong-Gang[1,2,3], WANG Shi-Wei[1,2]

(1. State Key Laboratory of High Performance Ceramics and Superfine Microstructure, Shanghai Institute of Ceramics, Chinese Academy of Sciences, Shanghai 200050, China; 2. Chinese Academy of Sciences Key Laboratory of Transparent and Opto-functional Advanced Inorganic Materials, Shanghai Institute of Ceramics, Chinese Academy of Sciences, Shanghai 200050, China; 3. University of Chinese Academy of Sciences, Beijing 100039, China)

Abstract: Alumina/carbon black foam was prepared by mechanical foaming and aqueous gelcasting and used as precursor for the production of AlN powder. The foam with large open pores ensures homogeneous solid-gas reaction during carbothermal reduction-nitridation (CRN) process. Further, the solid-gas contact is enlarged by oppositely feeding the foam and nitrogen in a vertical furnace. Solid-gas reaction efficiency of the CRN process was greatly enhanced when total porosity of the foam was ≥80%. XRD results revealed that γ-Al$_2$O$_3$ transformed to α-Al$_2$O$_3$ and then was carbothermal reduction-nitridationed to be AlN phase. AlN powder with an average particle size of less than 1 μm was synthesized at 1650℃ and contained 32.9wt% nitrogen.

Key words: chemical preparation; porosity; carbothermal reduction; aluminum nitride

Aluminum nitride (AlN), as an excellent material in semiconductor packages and heat sink, has attracted considerable attention in recent years, due to its outstanding properties, which include high thermal conductivity, low coefficient of thermal expansion that is similar to silicon, good resistance to thermal shock, high electrical breakdown strength and non-toxicity[1-5]. For such applications, it is critical to synthesize high-quality AlN powder to meet the demand of producing high performance AlN ceramics.

At present, AlN powder was synthesized by two primary processes: direct nitridation of Al powder and carbothermal reduction-nitridation (CRN) of Al$_2$O$_3$[6-7]. Compared with direct nitridation, the CRN process is more appropriate to synthesize AlN powder since it results in products with more attractive properties such as high purity, fine grain, uniformity, sinterability, and stability against humidity[8-10]. Nevertheless, the CRN process has some disadvantages, which include long reaction time, high nitridation temperature[11], and inhomogeneous solid-gas reaction because of N$_2$ diffusion from the surface to inside of powder stack. Investigations have been done to lower the synthesis temperature and reduce the fabrication cost. For example, Chu, et al[12] synthesized AlN nanoparticles by CRN using a combustion synthesis precursor derived from aluminum nitrate, glucose, and urea mixed solution. The precursor powder was transformed into phase-pure AlN at 1500℃. Lee, et al[13] obtained nanometer AlN powder with an average size of

20 nm above 1400℃ by a modified CRN route from aluminum oxide/carbon composite powder which prepared by spray pyrolysis. In addition, some additives were used to promote the reaction rate. Komeya, et al[14] studied the effect of CaF$_2$, Y$_2$O$_3$ and Yb$_2$O$_3$ additives on the nitridation reaction and concluded the degree of reaction promotion was in the order: CaF$_2$>Yb$_2$O$_3$>Y$_2$O$_3$. However, problems of CRN still exist, such as the inhomogeneous solid-gas reaction in the Al$_2$O$_3$/C powder stack, and powder loss during vacuum pumping and N$_2$ flow. To the best of our knowledge, there were no research reports on solving these issues.

Recently, ceramic foams with an open cell and controlled porosity have been prepared by mechanical foaming and gelcasting[15-16]. They have potential applications on gas or liquid filters or catalyst supports because of the large specific surface area of the porous structure[17]. In this work, Al$_2$O$_3$/C foam was fabricated by mechanical foaming and gelcasting. The foam with porous structure that ensures N$_2$ diffusion sufficiently was used as precursor to synthesize AlN powder by CRN process. We attempt to solve the issues of inhomogeneous solid-gas reactions and powder loss of the CRN process by using this novel way. Meanwhile, we design a vertical furnace to further enlarge solid-gas contact by oppositely feeding the foam and nitrogen (N$_2$). The effect of porosity of Al$_2$O$_3$/C foam on the nitridation rate was investigated. In addition, the effects of temperature on the nitridation rate and on the particle morphology of the powder were studied.

1 Experimental Procedure

The γ-Al₂O₃ powder (average particle size, 20 nm; specific surface area, 120 m²/g; Dalian Hiland Photo-electric Material Co., Dalian, China) and carbon black (average particle size, 18 nm; specific surface area, 226 m²/g; Cabot Co., Boston, America) were used as raw materials. A water-soluble copolymer of isobuthylene and maletic anhydride (1:1) with an average molecular weight of 55000–65000 (Isobam104#, Kuraray; Osaka, Japan) was used as both dispersant and gelling agent[18]. Iso-bam600AF (Kuraray; Osaka, Japan), which have a similar structure to Isobam104# and one-tenth molecular weight of Isobam104#, was used to increase the dispersing ability[19]. A commercial surfactant solution Emal TD (triethanolamine laurylsulfate, with 40% active content, Kao Chemical Co., Tokyo, Japan) was selected as the foaming agent.

A weight ratio 0.43 of C/Al₂O₃ (slightly larger than the theoretical value (~0.36)), was optimized to guarantee full conversion of Al₂O₃ to AlN[1]. Slurries were prepared by ball-milling the starting materials including Al₂O₃ powder, carbon black, deionized water, Iso-bam104# and Isobam600AF (named as Ib104 and Ib600, hereafter). The mixture was milled in a nylon container for 12 h using Al₂O₃ media. Then, Emal TD was added into the mixed slurry, which was then vigorously stirred for 3 min to generate foams. The foamed suspension was then poured into a mold to gel at room temperature in air. After demolding and drying at 110℃ for 12 h, Al₂O₃/C foam was obtained.

Zeta potential values of the slurries were measured by electrophoretic mobility (ZetaPlus, Brookhaven, NY). The pH were adjusted by sodium hydroxide and hydrochloric acid solutions. Rheological behaviors of the slurries were measured using a stress-controlled rheometer (Physica MCR301, Anton Paar, Graz, Austria). The shear rate was in the range of 1–1000 s^{-1}. The microstructures of Al₂O₃/C foams were observed by scanning electron microscope (SEM, JSM-6390LV, JEOL, Tokyo, Japan).

The total porosity (P) and open-pore ratio (P_a) of foams were measured by the Immersion Method after the immersion of foams in kerosene for 24 h. The expressions are shown as follows:

$$P = 1 - \frac{m \times d_m}{(m_1 - m_2)\rho_t} \qquad (1)$$

$$P_a = \frac{m_1 - m}{m_1 - m_2} \times 100\% \qquad (2)$$

Where m and m_1 are the masses before and after immersing into kerosene respectively, m_2 is the mass measured during the immersion in kerosene, and d_m and ρ_t are

the density of kerosene (0.80 g/cm³) and theoretical density of dense body which was calculated to be 2.79 g/cm³, according to the content of γ-Al₂O₃ and carbon black (70wt% and 30wt%) and the theoretical densities of γ-Al₂O₃ (3.66 g/cm³) and carbon black (1.80 g/cm³).

The CRN experiments were carried out in a self-designed continuously vertical type furnace. Al₂O₃/C foam was added from the top feeder, and nitrogen gas was introduced into the furnace from a gas inlet near the bottom. This special design ensures sufficient contact between the foam and nitrogen gas, which enhances the efficiency of the CRN process. Al₂O₃/C foams with different porosities were heated at 1300-1650℃ in N₂ for 2 h-4 h. The flow rate of N₂ was 5 L/min with a N₂ pressure of 0.1 MPa. The residual carbon in the nitridation products was removed by heat treatment at 600℃ for 3 h in air.

The crystalline phase of the as-synthesized products was examined by X-ray diffraction (XRD, D8-Advance A25, Bruker Co., Karlsruhe, Germany) with Cu Kα radiation and at a scan speed of 0.1°/s. The AlN conversion fraction was determined using a calibration curve based on XRD peak intensities of AlN-Al₂O₃ mixture. The morphologies of the products were observed by scanning electron microscopy (SEM, Hitachi, S-4800, Tokyo, Japan). The amount of nitrogen and oxygen in the AlN powder was measured by Oxygen-Azote mensuration equipment (TC600C, Leco Co., Chicago, America).

2 Results and discussion

2.1 Preparation of Al₂O₃/C foams

Figure 1 shows the effect of Isobam on the Zeta potential of slurries (powder/water: 0.2 g/L). The isoelectric point of the alumina without Isobam was pH 8.8. With the addition of 0.4wt% Ib104 and 0.6wt% Ib600, the pH value decreased to 4.9. The isoelectric point of carbon black without Isobam was pH 9.9, whereas it moved to pH 6.3
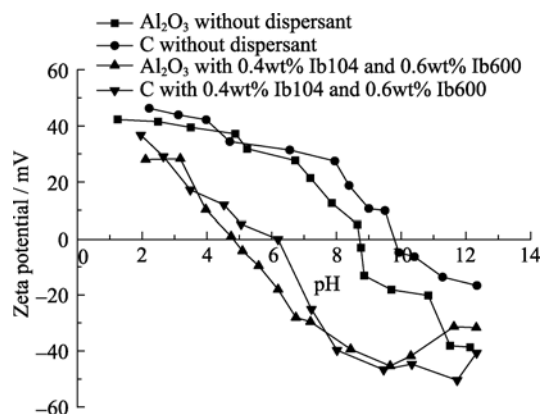

Fig. 1 Effect of dispersant on the Zeta potential of alumina and carbon black slurry

when the same amount of Isobam was added. For the alumina slurry, the Zeta potential changed to –40 mV at pH 8.8 with 0.4wt% Ib104 and 0.6wt% Ib600. As for carbon black, the Zeta potential was –43 mV at pH 9.9 after adding the same amount of Isobam. These results reveal that Ib104 and Ib600 can increase the dispersing ability of both alumina and carbon black in water.

To optimize the amount of the dispersant, the apparent viscosity of slurries were tested at room temperature (with different solids loading of 24wt% and 28wt%), as shown in Fig. 2. It can be seen that all slurries exhibited a shear-thinning behavior. It is also clear that with the increase of total Isobam content from 1.0wt% to 5.0wt%, the viscosity of the slurries observably decreases first, and then when the Isobam content increases from 5.0wt% to 6.0wt%, there is almost no obvious change in the viscosity. Furthermore, the viscosity of the slurries increased remarkably with increasing solids loading from 24wt% to 28wt%, resulting from the high specific surface area of carbon black and alumina powder. It is generally accepted that the slurry with low viscosity and good fluidity can offer a significant advantage for subsequent processes. Therefore, the slurry with 24wt% solids loading and 2.0wt% Ib104 plus 3.0wt% Ib600 was selected to fabricate Al_2O_3/C foams.

The influence of surfactant content on the foaming capacity of slurry with 24wt% solids loading, 2.0wt% Ib104 and 3.0wt% Ib600 is shown in Fig. 3. The foaming capacity is defined as the volume ratio of foamed slurry to the original one. The volume of the foamed slurry increased as the surfactant content increased. With the addition of 9vol% surfactant relative to the volume of the slurry, the volume of the foamed slurry was 7 times the original value; it did not increase after adding more surfactant. From the above, the foaming capacity of slurries can be controlled by adding surfactant with different contents. Thus, with constant stirring speed and stirring time, the Al_2O_3/C foams with different porosities were fabricated, as shown in Fig. 4, and the total porosity and open-pore ratio are shown in Fig. 5. Without surfactant and foaming, an Al_2O_3/C green body with 56% total porosity was obtained from the slurry with 24wt% solids loading, 2.0wt% Ib104 and 3.0wt% Ib600. Pores size was about 1 μm shown in the inset of Fig. 4a. After adding 2.0vol% surfactant, the Al_2O_3/C foam possessed a closed-cell structure with a total porosity of 70% (Fig. 4(b)) and open-pore ratio of 61%. As the surfactant content further increased to 2.4vol%, the total porosity and open-pore ratio increased to 80% and 73% respectively, and a large number of spherical cells interconnected by circular windows were observed. The cell size was less than 500 μm. The foam exhibited approximately spherical cells with no preferred orientation which was a typi

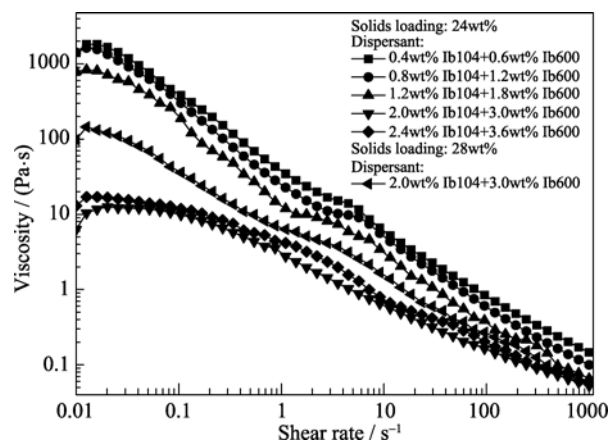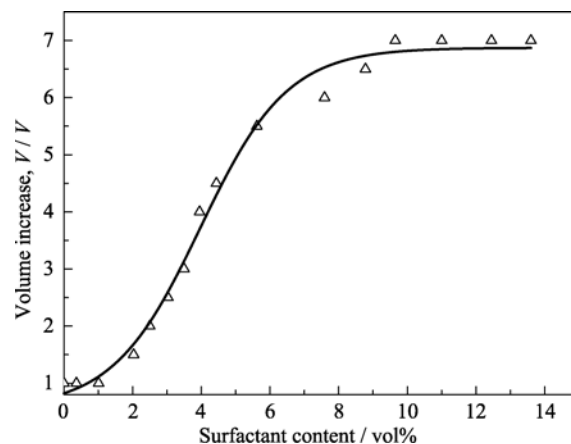Fig. 2   Rheological behavior of Al_2O_3/C slurries with different solids loading and dispersant content

Fig. 3   Evolution of the foaming capacity *versus* surfactant content

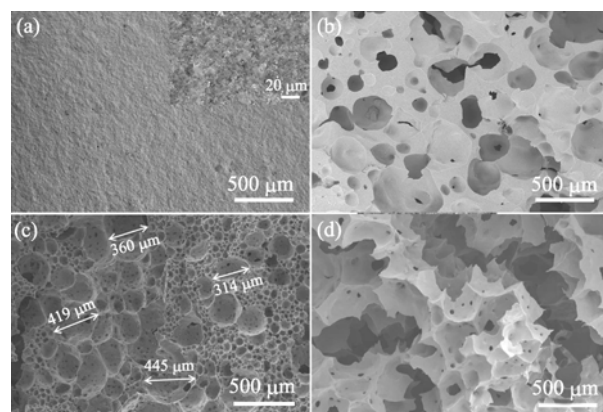Fig. 4   SEM micrographs of porous Al_2O_3/C foams with different surfactant additions
(a) 0vol%; (b) 2.0vol%; (c) 2.4vol%; (d) 4.0vol%

cal result of direct foaming method (Fig. 4(c))[17,20]. The foam prepared with 4.0vol% surfactant resulted in a total porosity of 90% and open-pore ratio of 82%. However, cracks happened after drying, as shown in Fig. 4(d).

2.2   Synthesis of AlN powder

To investigate the effect of total porosity of Al_2O_3/C foams on the nitridation rate, foams with total porosity of 56%, 70%, 80% and 90% were heated in the continuous synthesis furnace at 1600℃, and the AlN
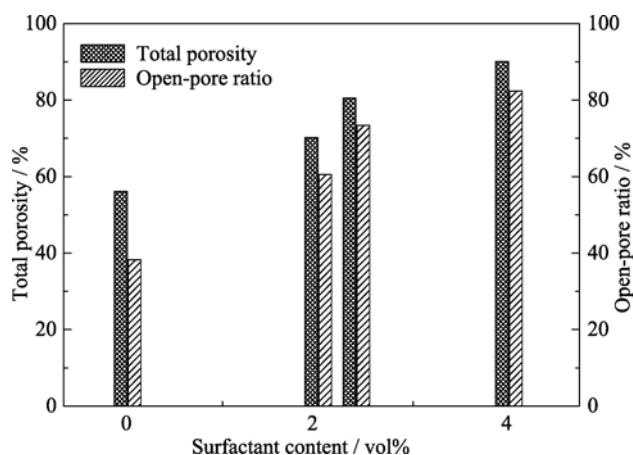
Fig. 5　Effects of surfactant content on total porosity and open-pore ratio of foams

Fig. 7　XRD patterns of the products by heating Al_2O_3/C foams at different temperatures

conversion fraction for different products are shown in Fig. 6. In general, AlN fraction remarkably increased with the porosity of foam. The minimum reaction time for achieving full conversion to AlN was 3.5 h for Al_2O_3/C foam with 56% total porosity. When the total porosity increased to 80% and 90%, the reaction time was decreased to 2 h. It can be easily concluded that the porous structure plays an important role in controlling the reaction rate. Compared with Al_2O_3/C powder stack, interconnected spherical cells with windows benefit N_2 diffusion rate and promote homogeneous solid-gas reaction. Hence, the reaction time needed for full conversion to AlN decreased as the porosity increased. Considering the fact that reaction rate of Al_2O_3/C foam with 80% total porosity was almost the same as that with 90% total porosity and the structure of the foam with 90% total porosity had cracks (Fig. 4(d)), Al_2O_3/C foam with 80% total porosity was chosen for the following studies.

Figure 7 shows XRD patterns of the products from the Al_2O_3/C foam with 80% total porosity heated at different temperatures in the range of 1300−1650℃ for 2 h. As shown, at 1300℃, only α-Al_2O_3 phase was detected in the product. It implied that the nitridation
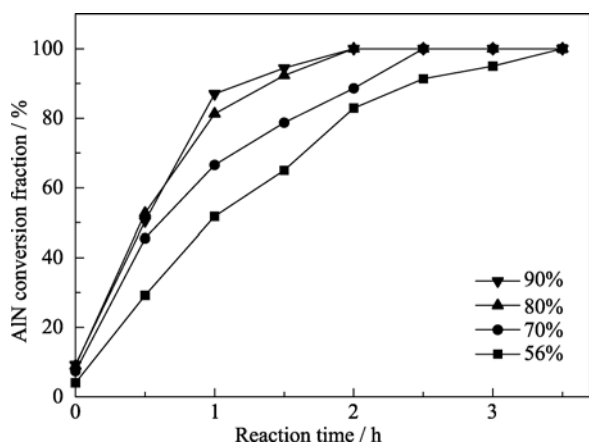
reaction of the foam has not occurred at this temperature. Products heated at 1400℃ and 1500℃ had diffraction peaks of both AlN and α-Al_2O_3. The α-Al_2O_3 peaks gradually weakened, while the AlN peaks strengthened as the reaction temperature increased. The phase-pure AlN was obtained when heated at 1550℃, 1600℃, and 1650℃, which indicated that the Al_2O_3 converted to AlN completely. Generally, during the CRN process, the higher the temperature, the stronger the intensity of the AlN peak is, revealing that the nitridation rate and the crystallinity of AlN were increased with reaction temperature. Moreover, no γ-Al_2O_3 diffraction peaks were observed during the nitridation process, suggesting that γ-Al_2O_3 converted to α-Al_2O_3 at first and then was nitrided to AlN.

The XRD patterns revealed that γ-α phase transformation occurred before CRN process. To investigated the effect of phase transformation on the structure of foam, the SEM photographs of foam with addition of 2.4vol% surfactant before and after calcined at 1300℃ for 2 h are shown in Fig. 8(a) and 8(b). It is distinct that the pore structure of foam was intact without any burst or collapse after calcined. That means that γ-α phase transformation had no impact on the foam structure.

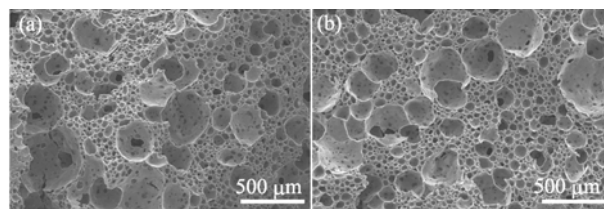To investigate the effect of temperature on the morphology of AlN powder, the morphologies of the

Fig. 6　Effect of porosity on nitridation rate under 1600℃

Fig. 8　SEM micrographs of foam with addition of 2.4vol% surfactant before (a) and after (b) being calcined at 1300℃ for 2 h
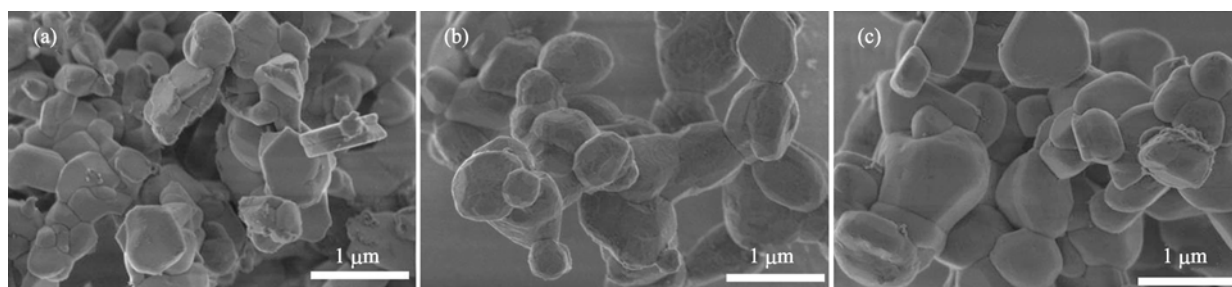
Fig. 9　SEM photographs of AlN powders synthesized at different temperatures for 2 h
(a) 1550℃; (b) 1600℃; (c) 1650℃

products heated in the range of 1550–1650℃ for 2 h were observed. SEM photographs of the relevant powders are shown in Fig. 9. Generally, the synthesized powder had an average particle size of less than 1 μm. However, the sphericity of AlN particles remarkably got better with the increase of temperature. At the low temperature of 1550℃, the powder was composed of irregular or disk-like shaped particles (Fig. 9(a)). Further increase in temperature produced spherical particles with a smooth surface (Fig. 9(b) and 9(c)). Combining this result with XRD patterns, it was concluded that the temperature has a great effect on nitridation rate and morphology of the AlN powder. The growth of AlN grain was improved as the temperature increased. The nitrogen and oxygen content in the AlN powder synthesized at 1550–1650℃ for 2 h are listed in Table 1. It clearly showed that the nitrogen content increased and the oxygen content decreased with increasing temperature. The powder synthesized at 1650℃ contained 32.9wt% nitrogen and 1.1wt% oxygen. The resulting powder with fine grains and high nitrogen content is a promising material to fabricate dense AlN ceramics with high thermal conductivity.

Table 1　Nitrogen and oxygen content of AlN powder synthesized at different temperatures

Element content/wt%	Reaction temperature/℃		
	1550	1600	1650
Nitrogen	31.9	32.4	32.9
Oxygen	1.6	1.2	1.1

3　Conclusions

In this work, an efficient and convenient technology which combines mechanical foaming and gelcasting with carbothermal reduction-nitridation was proposed for synthesizing fine AlN powder. Al_2O_3/C foams sufficiently ensured N_2 diffusion and solved the problem of inhomogeneous solid-gas reaction and powder loss of conventional CRN process. Al_2O_3/C foam composed of interconnected spherical cells with windows greatly enhanced the efficiency of solid-gas reaction of the CRN process. XRD patterns confirmed the phase transformation of γ-Al_2O_3 to α-Al_2O_3 occurred during CRN process. AlN powder synthesized at 1650℃ had fine grains (less than 1 μm) and high nitrogen content (32.9wt%).

Acknowledgements

References:

[1] SELVADURAY G, SHEET L. Aluminium nitride: review of synthesis methods. *Mater. Sci. Technol.*, 1993, **9(6):** 463–473.

[2] BACHELARD R, JOUBERT P. Aluminum nitride by carbothermal reduction. *Mater. Sci. Eng. A*, 1989, **109:** 247–251.

[3] VIRKAR ANIL V, JACKSON T BARRETT, CUTLER RAYMOND. Thermodynamic and kinetic effects of oxygen removal on the thermal conductivity of aluminum nitride. *J. Am. Ceram. Soc.*, 1989, **72(11):** 2031–2042.

[4] WEI P, QING Y, JUAN C. Mechanism of carbothermal synthesis of aluminium nitride. *Thermochim Acta*, 1999, **325(1):** 89–93.

[5] WANG Q, GE Y Y, CUI W, *et al*. Carbothermal synthesis of micro-scale spherical AlN granules with CaF_2 additive. *J. Alloys Compd.*, 2016, **663:** 823–828.

[6] IDE T, KOMEYA K, MEGURO T, *et al*. Synthesis of AlN powder by carbothermal reduction-nitridation of various Al_2O_3 powders with CaF_2. *J. Am. Ceram. Soc.*, 1999, **82(11):** 2993–2998.

[7] MOLISANI A L, YOSHIMURA H N. Low-temperature synthesis of AlN powder with multicomponent additive systems by carbothermal reduction-nitridation method. *Mater. Res. Bull.*, 2010, **45(6):** 733–738.

[8] ZAKORZHEVSKII V V, BOROVINSKAYA I P, SACHKOVA N V. Combustion synthesis of aluminum nitride. *Inorg. Mater.*, 2001, **38(11):** 1131–1140.

[9] CHU A, QIN M, JIA B, *et al*. Citric acid-assisted combustion-carbothermal synthesis of well-distributed highly sinterable AlN

nanopowders. *J. Am. Ceram. Soc.*, 2012, **95(8):** 2510–2515.

[10] WANG Q, CUI W, GE Y Y, *et al*. Preparation of spherical AlN granules directly by carbothermal reduction-nitridation method. *J. Am. Ceram. Soc.*, 2015, **98(2):** 392–397.

[11] LI C, KAO L, CHEN M, *et al*. Rapid preparation of aluminum nitride powders by using microwave plasma. *J. Alloys Compd.*, 2012, **542:** 78–84.

[12] CHU A, QIN M, JIA B, *et al*. Effect of urea on the size and morphology of AlN nanoparticles synthesized from combustion synthesis precursors. *J. Alloys Compd.*, 2012, **530:** 144–151.

[13] LEE S H, YI J H, KIM J H, *et al*. Preparation of nanometer AlN powders by combining spray pyrolysis with carbothermal reduction and nitridation. *Ceram. Int.*, 2011, **37(6):** 1967–1971.

[14] KOMEYA K. Synthesis of AlN Powder by carbothermal reduction-nitridation method. *J. Ceram. Soc. Jpn.*, 1993, **101(4):** 377–382.

[15] YANG Y, SHIMAI S, SUN Y, *et al*. Fabrication of porous Al_2O_3 ceramics by rapid gelation and mechanical foaming. *J. Mater. Res.*, 2013, **28(15):** 2012–2016.

[16] ZHANG X, SUN Y, SHIMAI S, *et al*. Effect of water-soluble epoxy resin on microstructure and properties of porous alumina ceramics by gel-casting. *J. Inorg. Mater.*, 2015, **30(10):** 1085-1088.

[17] SEPULVEDA P, BINNER J G B. Processing of cellular ceramics by foaming and in situ polymerisation of organic monomers. *J. Eur. Ceram. Soc.*, 1999, **19(12):** 2059–2066.

[18] YANG Y, SHIMAI S, WANG S. Room-temperature gelcasting of alumina with a water-soluble copolymer. *J. Mater. Res.*, 2013, **28(11):** 1512–1516.

[19] SUN Y, SHIMAI S, PENG X, *et al*. A method for gelcasting high-strength alumina ceramics with low shrinkage. *J. Mater. Res.*, 2014, **29(2):** 247–251.

[20] MAO X, SHIMAI S, WANG S. Gelcasting of alumina foams consolidated by epoxy resin. *J. Eur. Ceram. Soc.*, 2008, **28(1):** 217–222.

泡沫前驱体碳热还原氮化法合成氮化铝粉体

茅茜茜 [1,2,3]，李 军 [1]，张海龙 [2]，徐勇刚 [1,2,3]，王士维 [1,2]

(1. 中国科学院 上海硅酸盐研究所，高性能陶瓷和超微结构国家重点实验室，上海 200050；2. 中国科学院 上海硅酸盐研究所，中国科学院光功能无机材料重点实验室，上海 200050；3. 中国科学院大学，北京 100039)

摘 要： 本研究采用碳热还原氮化法(CRN)合成 AlN 粉体。以 γ-Al_2O_3 和炭黑为原料，采用直接发泡工艺与注凝成型相结合的方法制备出 Al_2O_3/C 泡沫，作为合成 AlN 粉体的前驱体。泡沫孔隙尺寸从几十微米到几百微米，总孔隙率 56%~90%。具有通孔结构的泡沫前驱体实现了原料内部各处的均匀的固–气反应，泡沫总孔隙率≥80%可显著提高 CRN 反应的速率。XRD 分析结果显示：CRN 过程中存在 γ-Al_2O_3 到 α-Al_2O_3 的相转变，反应起始温度在 1300℃以上，并在 1550℃反应完全。在 1650℃合成得到的 AlN 颗粒平均粒径不超过 1 μm，氮含量为 32.9wt%。

关 键 词： 化学制备；孔隙率；碳热还原；氮化铝

中图分类号： TQ174　　**文献标识码：** A